P-f Stability of 2030 Nordic Power System due to Non-Synchronous Generation

Das, Dwijasish; van Wageningen, N.A.; Rueda-Torres, José Luis; Gonzalez-Longatt, Francisco

DOI
10.1016/j.ifacol.2024.07.504

Publication date
2024

Document Version
Final published version

Published in
IFAC-PapersOnLine

Available online at www.sciencedirect.com

ScienceDirect

IFAC PapersOnLine 58-13 (2024) 332–337

P-f Stability of 2030 Nordic Power System due to Non-Synchronous Generation

Dwijasish Das * **N.A. van Wageningen** *
José-Luis Rueda-Torres * **Francisco Gonzalez-Longatt** **

* *Delft University of Technology (TU Delft), Delft, Netherlands (e-mails: d.das-1@tudelft.nl, j.l.ruedatorres@tudelft.nl).*
** *Loughborough University*

Abstract: The Nordic Power System is undergoing significant transformation and development in the coming years. A driving factor for this is the increased dependency on renewable energy sources and high voltage direct current transmission (HVDC). Various stability challenges due to the dynamics of reactive power - voltage (Q-V) balancing and active power - frequency (P-f) balancing seep into the system with such rise of non-synchronous generation (NSG). This paper investigates the projected impact of NSGs on the P-f dynamic performance of Nordic power system in 2030. As NSGs are systems with low inertia, power discrepancies lead to larger oscillations, higher Rate of Change of Frequency (RoCoF) and bigger maximum frequency deviation (MFD) values. To adderess these issues, Emulated Inertia (EI) control for wind turbines and Synthetic Inertia (SI) control for VSC-HVDC links are proposed in this paper. The simulation is carried out using DIgSILENT PowerFactory 2022 SP1 simulation software. The results obtained confirm the effectiveness of the proposed EI and SI methods to enhance frequency response and mitigate deviations.

Keywords: DIgSILENT PowerFactory, frequency stability, HVDC, non-synchronous generation, Nordic power system.

1. INTRODUCTION

The increased focus on renewable energy has led to substantial growth in wind generation systems and HVDC transmission. Wind generation and HVDC imports constitute forms of Non-Synchronous Generation (NSG) as they are decoupled from the grid by power electronic converters. Displacing conventional synchronous generation by NSG lowers the inertia and causes heterogeneity of power system with power being fed from various types of sources Ulbig et al. (2014). Besides, increasing NSG, especially in power supply shares above 50%, challenges the effectiveness of primary and secondary stages of active power-frequency control to mitigate undesirable values of the rate-of-change-of frequency (RoCoF) and the maximum frequency deviation (a.k.a. frequency Nadir/Zenith), and to quickly restore the frequency, respectively Nordic TSOs (2016).

This paper presents a dynamic digital model that is developed to investigate dramatic changes in the frequency performance of the Nordic Power System considering the evolution of its NSG by year 2030. The model is created by using generic component dynamic (differential-algebraic) representations. Time domain simulations are conducted in the futuristic model of the Nordic Power system for a situation of low demand combined with 60% NSG (due to projected high penetration of wind power generation and HVDC imports). The reminder of the paper includes an overview of the model development in Section 2, numerical simulations and their evaluation in Section 3, and a summary of concluding remarks in Section 4.

2. DEVELOPMENT OF THE DYNAMIC MODEL

A futuristic situation for the dynamics of the Nordic Power System is created by using the functionalities for root-mean-square (RMS) modelling and simulation provided by DIgSILENT PowerFactory.

2.1 General Modeling Assumptions

The dynamic digital model builds on a previously developed model, which was originally implemented for power flow calculations in year 2020 Aas (2016). The focus of the work presented in this paper is to significantly upgrade the model to include generic dynamic models, including the addition of future wind power plants and HVDC links. Based on the reference simulations presented in Aas (2016), different scenarios were created for future power flow profiles, such as high renewable generation and high imports/export of power through HVDC links in 2030. The model presented in Aas (2016) is a reduced size model consisting of 31 nodes at transmission voltage. Namely, the system has four transmission voltage levels (400 kV, 300 kV, 220 kV and 22 kV). The nominal voltage of the transmission backbone in Norway is 420 kV instead of 400 kV as defined in the model. The loads, generators and SVCs compensate for this difference by applying a voltage set point of 1.05 p.u.. Besides, all synchronous generators operate in the constant voltage mode, which is set at 1.05 p.u.. The lines are presented by equivalent models. The loads are modeled as 30% constant power, 30% constant current, and 40% constant impedance models by

10.1016/j.ifacol.2024.07.504

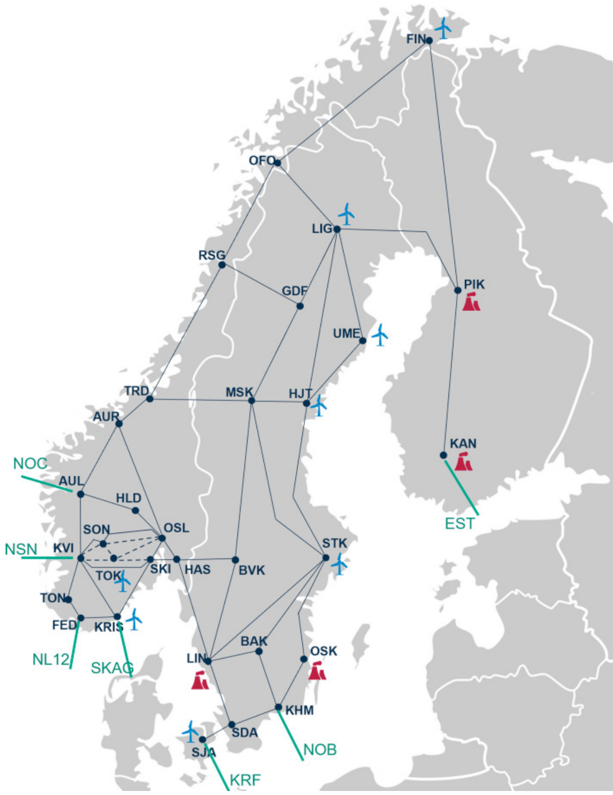

Fig. 1. Distribution of generation types in the 60% NSG scenario van Wageningen (2022).

using the classical voltage-dependent approximation for numerical simulations. Detailed descriptions of the generic component models and their corresponding parameter as implemented in PowerFactory can be found in DIgSILENT GmbH (2021).

2.2 Definition of a Future Operational Scenario

To evaluate the frequency response of the future Nordic Power System under low-system inertia, the model described in Aas (2016) is adapted. The overview is shown in Fig. 1. Specifically, a scenario is defined where 60% of the power demand is met by NSG, which does not contribute to the initial inertial frequency response of the system, and it is defined by the following rule:

$$\%NSG = 100\% \frac{P_{NSG} + P_{HVDCimport}}{P_{Demand} + P_{HVDCexport}} \quad (1)$$

Three power plant types are included: hydro, thermal (gas and nuclear) and wind. The Mid-term Adequacy Forecast (MAF) by ENTSO-E is used to define estimated evolutions of the capacity per area in MW ENTSO-E (2020). Wind production is expected to increase in the northern part of Sweden and Norway FINGRID, Landsnet, Svenska Kraftnät, Stattnett, and Energinet.dk (2019). The current considerable share of wind power in Sjælland (SJA), or East-Denmark will continue to grow Nordic Council of Ministers (2015). Tokke (TOK), Kristiansand (KRI) and Stockholm (STK) increase the percentage of NSG to 60 % FINGRID, Landsnet, Svenska Kraftnät, Stattnett, and Energinet.dk (2019). Oskarhamn (OSK) is an existing nuclear plant. In Finland, Nuclear and Biomass will continue to have a significant share

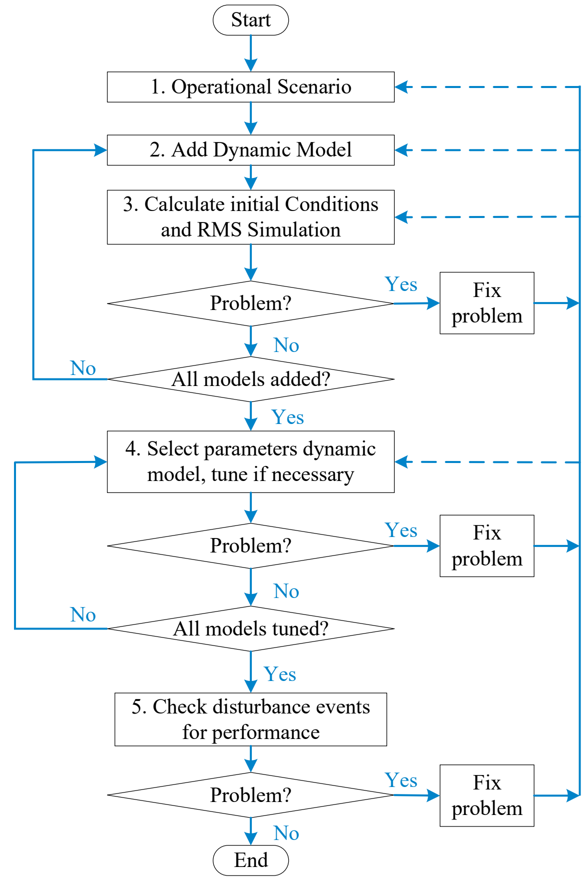

Fig. 2. Flowchart of procedure to modify the base scenario to the 60% NSG scenario

of installed capacity Nordic Council of Ministers (2015). Consequently, Kangasala (KAN) is modelled as a nuclear plant and Pikkarala (PIK) is modelled as Biomass. As the phasing out of nuclear energy in Sweden is only expected to start after 2030, Lindome (LIN) is modelled as a Nuclear plant.

2.3 Modifications of the Base Model

To reach the 60% NSG scenario, multiple modifications of the base model are made. These are discussed as follows.

Modelling Procedure Fig. 2 presents the process to modify the base scenario.

1. Some of the synchronous generators are replaced with the wind turbines, the VSC-HVDC terminals are replaced by static generators and the LCC-HVDC links are modeled as negative loads. In the base system, the generators are loaded till 20%. The number of generators is therefore decreased to a loading of 80%. The change in transformer losses and the operational set-points of wind turbines closer to a power factor of 1 resulted in different bus results. Set-points of loads were used to maintain voltages.

2. The dynamic models of the different generation types were added one a time. Afterward, the dynamic models were checked for their dynamic performance for small increases of load and tuned if necessary.

3. To check if the dynamic models are correct, all state variables are initialized using the 'Initial Conditions' cal-

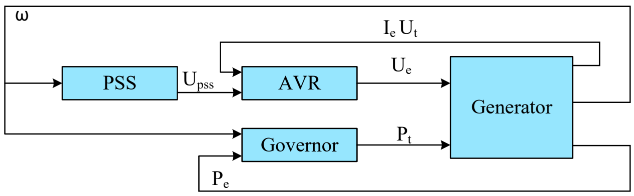

Fig. 3. Composite model of Synchronous Generator with Common Models for PSS, AVR and Governor

culation (steady state Loadflow calculation). Additionally, the RMS simulation is run for 5 seconds without an event to see if the initialization results in constant powerflows.

4. The parameters of the dynamic models are tuned with a small frequency event.

5. Problems in the system became only apparent during the investigation into the critical disturbances. The model was modified iteratively. Problems had to be solved in different domains and were discovered at different stages. A change in one location of the system influenced other areas and testing for one disturbance does not ensure performance for other disturbances. As a result, large part of the process was based on trial and error. The nodes with wind generation have a nominal setpoint of 6 MW. The synchronous generators are not all loaded to 80-100%, which would be a better representation. This was needed to maintain rotor angle stability.

Synchronous Generators The generation type and the size, or rated power, determines the amount of inertia a synchronous generator can offer. The inertia values used in the model are taken from E. Ørum and M. Kuivaniemi (2015). The synchronous generator is adjusted with values taken from the equipment type 255 MVA ST taken from the DiGSILENT library in the RMS simulation tap. Furthermore, the reactive power limits were set at the maximum value.

Dynamic Model for Synchronous Generators The Composite Frame with the interactions between the AVR, PSS and Governor are shown in Fig. 3. The function of the governor is to maintain the frequency by adjusting the power output with a predefined droop value. The AVR is responsible for the voltage control. By adjusting the excitation voltage, the voltage at the output of the generator is controlled. With the lag between the excitation voltage and voltage at the output, a strong acting AVR can lead to oscillations, which can be dampen by adding a PSS.

The governor of the Hydro generators is modelled as the HYGOV model available for PSSE Software (Power System Simulator for Engineering). The permanent droop (R) is the primary control parameter that adjusts the opening of the gate proportionally to difference in speed of the generator. The temporary droop (r) has the function to stabilize the output of the governor system, to reduce the overshoot caused by R. The water flow does not react instantaneously to changes in the mechanical changes of the gates. This lag is described by the water starting time (Tw). The governor time constant (Tr) is recognized as a damping time and is typically around around 5Tw. The Servo Time constant (Tg) relates to the time it takes the servo gates to close and open. The effect of these parameters is shown in Fig. 4. The AVR of the Hydro generators is modeled as a simplification of the DC1C excitation system of IEEE PES (2006). It includes an overexcitation limiter (OEL) to avoid windups and a PID of the AVR controller. Performing criteria for small signal and large signal stability problems is provided by IEEE (2014). The PSS of the Hydro generators has one input, i.e., the rotor speed and the range of values defined by IEEE (2014) (also used for thermal generators).

Fully Rated Converter Wind Model At 8 Nodes a wind turbine replaces the synchronous generator, using the General Template 'DIgSILENT FullyRatedConv WTG 6.0MW 50Hz'. Information for this template can be found in DIgSILENT (2020). The WT is modeled as a static generator with an extra transformer. The required power output is reached by increasing the number of parallel transformers and static generators. This model was chosen because it gave no problems with initialization, the RMS simulation without events gave a steady input after 5 seconds. The wind turbines operate at nominal power and power factor. The controller is set on 'Const Q'.

During the dynamic control, the PQ controller and the current controller adjust their output with the goal to keep the power values close to initial values. Furthermore, the Phase Lock Loop (PLL) block measures and adjusts the signals for the frequency and the angle phi. The control blocks in the composite models function as follows: The PQ control uses these measurements and compares them with reference values and adjusts them with PI control. If the voltage deviation is higher than a predefined value, an extra gain is added to the Q signal. The reference value for P can be adjusted by the signals from the Active power reduction blocks. The direct, quadratic and combined current, and internal voltage are limited if predefined values are reached. The current controller calculates the 1st sequence voltage references. The measured two-phase currents are transformed into two static currents in rotating frames. The PLL contributes the position of the direct axes compared to the voltage angle. Then, a PI controller adjusts these currents with the reference signals from the PQ controller before it is calculated back to two phase voltage values. The Active Power Reduction block decreases the power reference during over frequency events. The Emulated Inertia block completes the frequency control for the wind turbine as it works for under frequency events. The PQ current has a control loop for voltage support which has a deadband. The voltage dead band (deltaU) determines when this control starts. There are two control possibilities: following the transmission code 2007 (a) or SDLWIndV in 2007 (b). According to Statnett (2023) wind parks with a production of 10 MW or higher should partake in voltage stability. However, changing the deadband parameter deltaU to 0 resulted in initialization problems of the wind turbine. Fig. 5(a) shows the effect of decreasing the deadband deltaU on the voltage magnitude. For deltaU = 0.1, the voltage deviation is not bigger than the deadband and the reactive current is not changed. Only in this case, the voltage does not decrease and, in the other cases, large spikes can be seen in the voltage. The effect of changing the deadband parameter deltaU on the frequency can be seen in Fig. 5(b). Changing the voltage deadband results in volatile frequency characteristics. Note

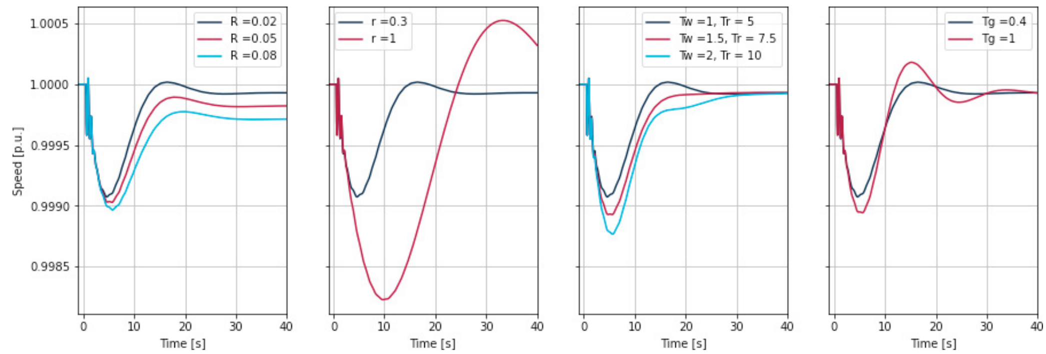

Fig. 4. Speed time responses of Hasle for a sudden load increase of 10% in Oslo for different HYGOV parameters

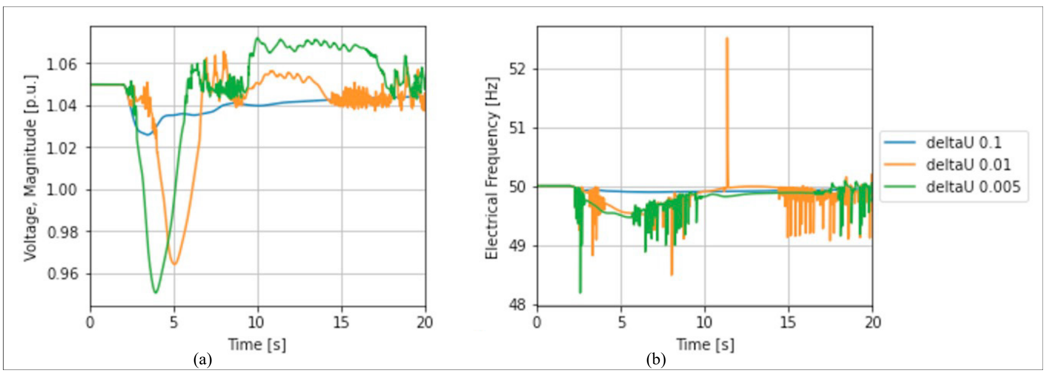

Fig. 5. Effect of different values of deadband deltaU on (a) voltage magnitude and (b) frequency.

that without the voltage support, the reactive power of all WTs are set at zero. The deadband parameter deltaU is set to the default parameter 0.1.

HVDC Links The LCC-HVDC links were modelled as negative loads. The active and reactive powers were taken from the output of the LCC-HVDC links from the base model. The loads were modelled as 100% constant power load, which acts as a fully static during RMS simulations. VSC-HVDC links are represented by the model "HVDC MMC 2-Terminal LInk (RMS Balanced)" from DIgSILENT library. The rated voltages and powers per HVDC link were taken from Aas (2016). For loadflow calculations, VSC-HVDC is modeled by means of two static generators as the HVDC link terminals. Fig. 6 shows the frame for HVDC link. The value for the active power flow is determined in a separate Quasi-Dynamic Simulation model. HVDC converter 1/A controls the active power and sets the P setpoint. HVDC converter 2/B is modelled as the converter controlling the DC voltage. These signals are taken by the HVDC-link control block and the DC voltages and currents at both sides are calculated using the user defined values. The HVDC terminals then control these values to specific needs.

A rough summary of the VSC-HVDC converter control can be seen in Fig. 7. The measurement and signal processing collects and calculates the signals for voltage and current as well as the phase angle and frequency from the PLL. The protection block then checks whether the voltages, currents and frequencies are in between the operational limits and opens circuit breakers if necessary. In the Outer Loop Dynamics, the setpoints for active power and re-

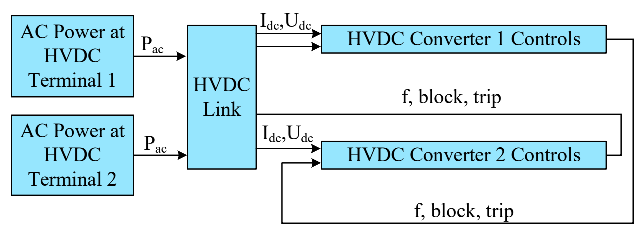

Fig. 6. Composite Frame for VSC-HVDC link.

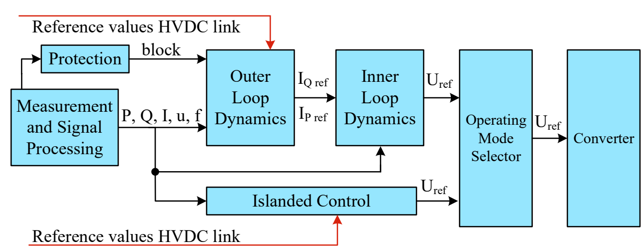

Fig. 7. Summary of VSC-HVDC converter control.

active power are created and it consists of the following models: Emergency Power Control can adjust the active power reference when triggered. The Synthetic inertia control block adjusts the power reference proportional to the RoCoF to mimic inertial response from synchronous generators. Frequency Sensitive Mode adjusts the active power reference with a specified power frequency characteristic. Power Oscillation Damping's function is to damp power system oscillations (both active and reactive power) with a lead-lag control block. The active power references are combined with the power measurement in the P/Vdc control block. It can either regulate the DC voltage or the

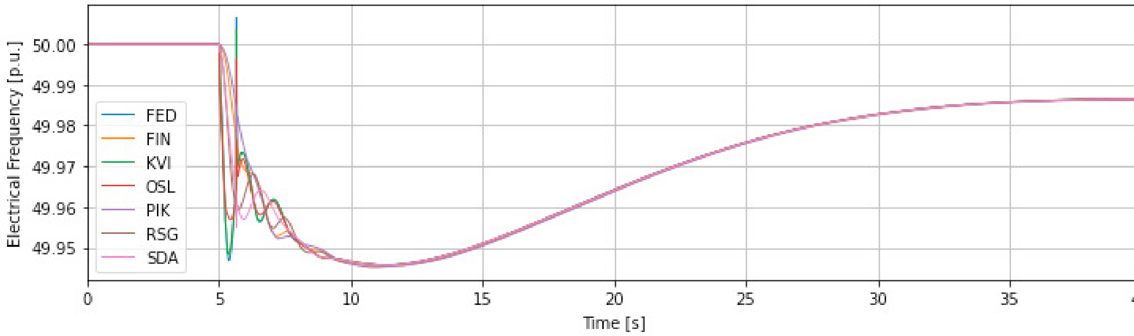

Fig. 8. Frequency response at geographical dispersed locations after a sudden load event of 10% at OSL.

active power. PI controllers adjust the measured P/Vdc to the reference values. For the high import scenario, the converters connected to the Nordic Power System were first controlling the active power. However, this led to initialization problems. The output of the converter controlling the P is more robust and led to a more stable initialization.

The Q/Vac Control regulates either the reactive power or the AC voltage in the same manner as the P/Vdc block. The converters connected to the Nordic Power System and the ones connected to the external grids regulate the reactive power. It is operating in droop control mode, so the reactive power is influenced by the AC voltage. This helps stabilizing the voltages in the Nordic Power System and gave a quicker steady state in the RMS simulation. During a system fault, the q control is adjusted proportional to the voltage drop to help with voltage regulation. In the Inner Loop Control, firstly, the Current Limiter checks the reference values and decreases it if it is above predefined limits. The Current Controller regulates the measured direct and quadratic currents and translates them into reference voltage signals. The signal is again checked if it's not too high in the Output Limiter block. The Islanded Control circumvents the inner and outer controls, but uses the signals to regulate the active and reactive powers and sends it to the Operational Mode Selector which selects which of the signals to send to the converter according to which mode is in service.

3. EVALUATION 60% NSG SCENARIO TO A SMALL FREQUENCY EVENT

To show the dynamic performance of the system, a sudden load increase of 10% at Oslo (OSL) is simulated at t = 5 s. This results in a power deficiency of 374 MW. The total load in the system is 36.2 GW. The electrical frequency at FED, OSL, PIK, RSG and SDR is shown in Fig. 8. As can be seen, rotor swings occur close to the fault, in PIK the rotor swings are not visible. The figure indicates different inertia levels of the areas by various RoCoF at the start. The frequency dip is reached at 7 seconds, whereas the quasi steady state is reached after 25 seconds after the fault. This is in the range described by IEEE (2013).

3.1 Dynamic Response of Hydro Synchronous Generators

Fig. 9(a) shows the frequency response of the hydro generators. The frequency response is similar, due to their proximity. There is a small overshoot in the first swing. Fig. 9(b) shows the voltage characteristic of the hydro generators. Voltage oscillations in the first few seconds are quickly restored. The initial voltage is not restored, but a constant voltage level is reached after 40 seconds.

3.2 Dynamic Response of Thermal Synchronous Generators

Fig. 10(a) shows the frequency response of the thermal generators. The frequency response differs in the first couple of seconds, due to the distance between them. The voltage response of the busses with thermal generation is depicted in Fig. 10(b). Compared with the hydro generation models, voltages take longer to get to the quasi steady state and there is an overshoot.

3.3 Dynamic Response of Static Generators with a Dynamic Wind Control

Fig. 11(a) depicts the frequency of the busses with WT. Compared to the Fig. 8 and 9, the frequency in the first few seconds after the event show many oscillations and high values of RoCoF. This happens because there is no natural inertia at busses with wind. Fig. 11(b) shows the voltage response of all wind turbines. KRI and TOK are smaller wind turbines that are surrounded with synchronous generators and the voltage at those points are quickly restored. UME experiences the biggest voltage dip, as it is solely connected with nodes that have wind generation. The wind turbines do not partake in voltage regulation. The control system is only regulating the reactive power output to remain at initial value.

4. CONCLUSIONS AND RECOMMENDATIONS

The paper highlights the critical challenges that appear along with the integration of renewable energy sources and HVDC. The impact of NSG on the frequency stability is studied and EI control for wind turbines and SI control for VSC-HVDC links are proposed to mitigate frequency deviations increasing the system resiliency. As NSG lacks inertia, it leads to larger oscillations, higher rates of change of frequency (RoCoF), and bigger maximum frequency deviation (MFD) values, challenging traditional frequency control mechanisms. The effectiveness of the proposed control methods is validated based on simulations. Based on the findings, the paper offers recommendations for improving the frequency stability of the Nordic Power System,

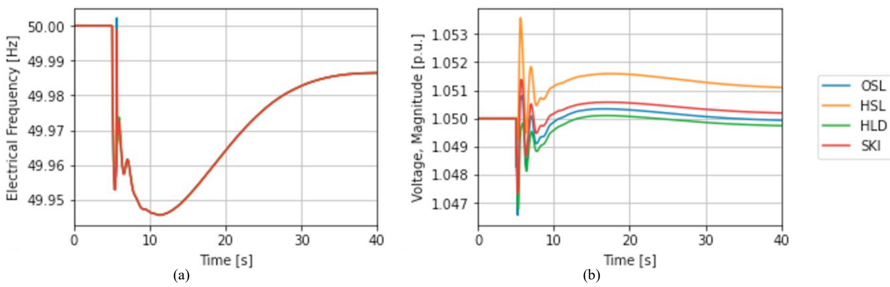

Fig. 9. a) Frequency response of OSL, HSL, HLD and SKI after a 10% load increase in OSL b) Voltage response of OSL, HSL, HLD and SKI after a 10% load increase in OSL.

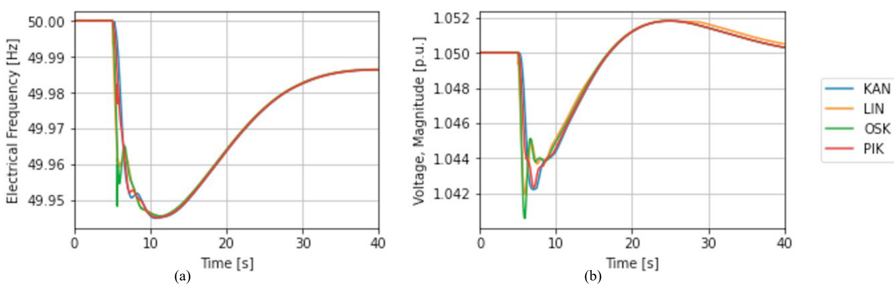

Fig. 10. a) Frequency response of KAN, LIN, OSK and PIK after a 10% load increase in OSL b) Voltage response of KAN, LIN, OSK and PIK after a 10% load increase in OSL.

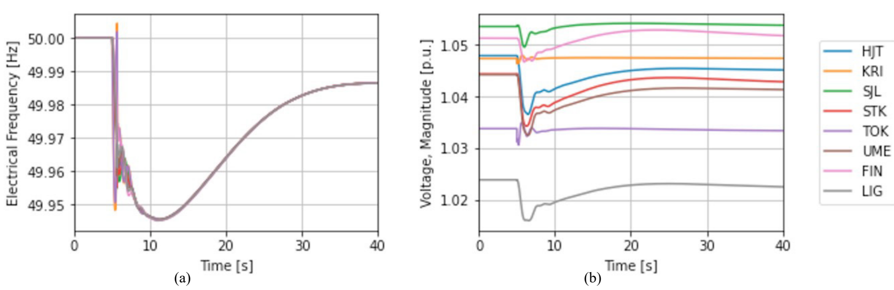

Fig. 11. a) Frequency response of static generators with wind models after a 10% load increase in OSL b) Voltage response of static generators with wind models after a 10% load increase in OSL.

such as fine-tuning control parameters, enhancing grid resilience, and exploring additional measures to address frequency deviations effectively. Such measures can help develop a strong heterogeneous grid.

REFERENCES

Aas, E.S. (2016). Simulation model of the future nordic power grid considering the impact of hvdc links.

DIgSILENT (2020). Technical reference digsilent fully rated converter wind turbine templates. *DIgSILENT GmbH PowerFactory 2021, Gomaren, Germany, Tech. Rep.*

DIgSILENT GmbH (2021). Technical reference general load. *PowerFactory 2021 Brochure*, 1–28.

E. Ørum and M. Kuivaniemi (2015). Nordic report: Future system inertia. *Entso-E*, 1–58.

ENTSO-E (2020). Mid-term adequacy forecas 2020 dataset.

FINGRID, Landsnet, Svenska Kraftnät, Stattnett, and Energinet.dk (2019). Nordic grid development plan 2019. 83.

IEEE (2013). Dynamic models for turbine-governors in power system studies. *IEEE Task Force on Turbine-Governor Modeling Technical Report PES-TR1*, 1–117.

IEEE (2014). Ieee guide for identification, testing, and evaluation of the dynamic performance of excitation control systems. *IEEE Std 421.2-2014 (Revision of IEEE Std 421.2-1990)*, 1–63.

Nordic Council of Ministers (2015). Capacity adequacy in the nordic electricity market.

Nordic TSOs (2016). *Challenges and opportunities for the Nordic Power System.*

PES (2006). Ieee recommended practice for excitation system models for power system stability studies. 1–85.

Statnett (2023). Funksjonskrav i kraftsystemet (FIKS 2012) publisert .

Ulbig, A., Borsche, T.S., and Andersson, G. (2014). Impact of low rotational inertia on power system stability and operation. *IFAC Proceedings Volumes*, 47(3), 7290–7297. doi:https://doi.org/10.3182/20140824-6-ZA-1003.02615. 19th IFAC World Congress.

van Wageningen, N. (2022). Frequency support of non-synchronous generation in the nordic power system in 2030. Masters Thesis, Delft University of Technology.